

Nonlinear magneto-optical effects in Ba vapor

I. Novikova,^{1,2} A. Khanbekyan,³ D. Sarkisyan,³ and G. R. Welch¹

¹*Department of Physics and Institute for Quantum Studies,
Texas A&M University, College Station, Texas 77843-4242*

²*Harvard-Smithsonian Center for Astrophysics, Cambridge, Massachusetts, 02138*

³*Institute for Physical Research, Armenian Academy of Science, Ashtarak-2 378410 Armenia*

(Dated: October 31, 2018)

We report the first measurements of linear and nonlinear magneto-optical polarization rotation on an intercombination transition of Ba vapor ($\lambda = 791.1$ nm). We observe a maximum polarization rotation angle in Faraday configuration of 15 mrad, accompanied by suppression of absorption. A theoretical treatment of the nonlinear Faraday effect in the limit of a strong interacting light field is developed.

PACS numbers: 33.55.-b,42.50.Gy

In the last few decades, nonlinear magneto-optical effects (NMOE) have been studied thoroughly in various experimental configurations, and they have been used or proposed to be used for many practical applications, including precision metrology and fundamental symmetry tests (for a review see Ref. [1]). The majority of experiments, however, are focused on the interaction of resonant light with alkali atoms like Rb, Cs and Na. There are only a few publications reporting studies of NMOE for alkaline-earth atoms: the study of nonlinear Faraday and Voigt effects in Sm [2, 3] and the study of the nonlinear Faraday effect in the regime of strong magnetic fields in Ca [4].

We present here the first (to our knowledge) measurements of nonlinear magneto-optical polarization rotation in Ba vapor for laser radiation resonant with the $6s^2 \ ^1S_0 \rightarrow 6s6p \ ^3P_1$ intercombination transition ($\lambda = 791.1$ nm). This transition is of particular interest since the angular momentum of the ground state is zero, and the nonlinear effects are due to the interference of the magnetic sublevels of the excited sublevels in a V level scheme. It should be noted that although there exists a number of theoretical calculations of nonlinear polarization rotation in $J = 0 \rightarrow J' = 1$ transitions [5, 6, 7], experimental results are very limited [3]. Coherence effects in a V -type level configuration have also been studied in regards to lasing without inversion [8, 9, 10], but with very little experiments focused on the dispersive properties of this system.

The interaction of linearly polarized light with the intercombination transition of Ba forms an ideal V scheme which cannot be realized in, for example, alkali atoms because of their richer Zeeman structure. It has been demonstrated that ground state coherence may be formed due to radiative coherence transfer if the ground state is degenerate even in the case of higher degeneracy of the excited state [11, 12, 13], which may obscure the observation of the coherence between excited states. It is also important that the radiative width of the excited state 3P_1 is small ($\gamma_r = 2\pi \times 100$ kHz) which is true for the majority of alkaline-earth elements. Thus, the coherence created between the excited state sublevels may

exist long enough to produce a noticeable nonlinear effect.

In addition, since the frequencies of the intercombination transition in Ba and the D_1 line of Rb are very close ($\Delta\lambda \approx 3$ nm) it is logical to expect resonant enhancement of the spin-exchange cross-section between atoms of the two species. Therefore, the study of linear and nonlinear effects in Ba should provide accurate information about the interaction with Rb atoms and vice versa. In this case Ba atoms may be used to monitor the properties of very dense Rb vapors.

In this paper we first present the experimental data for saturation absorption spectroscopy of Ba atoms. These data provide the necessary information about level structure of various Ba isotopes, and allow better calibration of the magnetic field. Then we study the linear and nonlinear Faraday effects for different experimental parameters. In the last section we analyze the observed experimental data using density matrix formalism.

I. EXPERIMENTAL SETUP

A. Sapphire Ba cell

In this experiment we use a sealed cylindrical sapphire cell (SC) containing pure Ba with birefringence-free windows made of garnet (YAG) crystal. This cell allows operation at high-temperature (up to 600°C on the windows). The length of the cell is $L = 102$ mm, with an inner diameter of 10.7 mm. The residual vacuum in the SC is $\sim 10^{-3}$ Torr.

Heating elements are placed closer to the windows to avoid condensation of Ba vapor on the windows of the SC and to prolong its useable lifetime. The temperature is then measured by two nonmagnetic thermocouples: one is placed next to the window so it detects the highest temperature of the SC, and the other is located in the central part of the cell to detect the lowest temperature. Both the SC and the heaters are surrounded by a thermoisulating material (“shamot”).

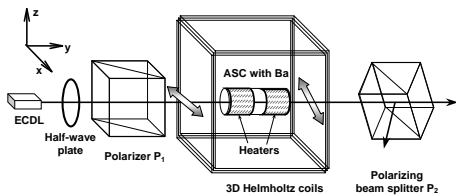


FIG. 1: Scheme of the experimental apparatus.

We conduct the experiment at two different temperatures of the SC: at 490°C (temperature on the window is 515°C), and at 540°C (temperature on the window is 560°C). There is no well-established dependence of Ba vapor pressure on its temperature, as it is noted in [14]. Below, we give the standard function describing this dependence, and the numerical values of the coefficients from different studies:

$$\log(p) = A + BT^{-1} + C \log T \quad (1)$$

where p is measured in Pa, and T is in K.

Reference	A	B	C
Hinnov <i>et al.</i> Ref. [15]	8.9	-8800	0
Alcock <i>et al.</i> Ref. [16]	17.411	-9690	-2.2890
Jacob <i>et al.</i> Ref. [17]	9.733	-9304	0

We need to point out that the values of atomic densities calculated using the various tabulated coefficients are not consistent with each other for our experimental temperatures. In the following we will use the most recent study of Jacob *et al.* [17] which gives the values of Ba atomic densities for our experiment to be $N = 3.3 \times 10^{11} \text{cm}^{-3}$ and $N = 1.8 \times 10^{12} \text{cm}^{-3}$. The data from [15] give values about 40% lower, whereas those of [16] give a Ba pressure an order of magnitude larger.

B. Experimental configuration

A simplified scheme of the experimental setup is shown in Fig. 1. We use an external cavity diode laser (ECDL), tuned to the vicinity of the $6s^2 \ ^1S_0 \rightarrow 6s6p \ ^1P_3$ intercombination transition of atomic Ba. The laser beam passes through a high-quality polarizer P_1 (to insure the quality of the linear polarization). A half-wave plate placed in front of the polarizer allows smooth control of the intensity of the laser beam at the SC. The cell (with the heaters and thermal isolation) is mounted in the center of triaxial Helmholtz coils to control the magnetic field within the interaction region. The system consists of three mutually orthogonal pairs of square coils in Helmholtz configuration, with the magnetic field inhomogeneity of ± 5 mG within a 10 cm cubical central region.

After traversing the Ba cell, the transmission and the polarization rotation are analyzed by using a polarization beam splitter (P_2 in Fig. 1) tilted at 45 degrees with respect to the polarizer P_1 . In this configuration the output signal of the two channels of the beam splitter

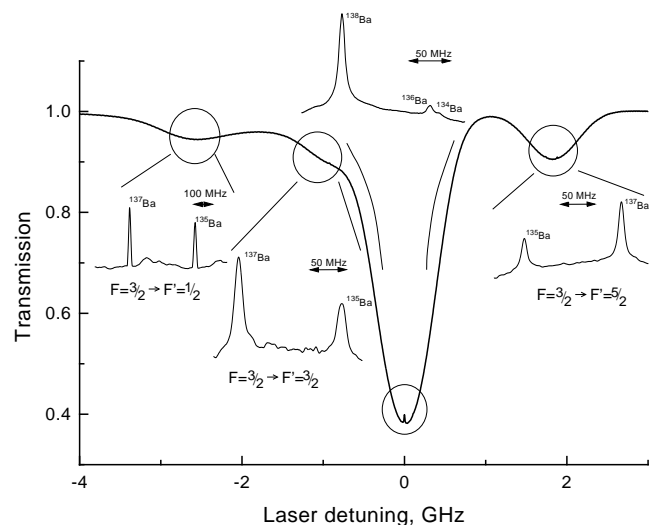


FIG. 2: Transmission spectrum of the laser field as its frequency is swept across the intercombination transition of Ba. *Insets*: the saturation absorption spectra for each absorption peak. The power of the probe and pump fields are $150 \mu\text{W}$ and 2mW respectively. The atomic density of Ba is $N = 1.8 \times 10^{12} \text{cm}^{-3}$.

are given by $S_{1,2} = \frac{1}{2} I_{\text{out}} (1 \pm \sin 2\phi)$, where I_{out} is the transmitted intensity of the laser beam, and ϕ is the polarization rotation angle.

II. EXPERIMENTAL RESULTS

A. Saturation absorption spectroscopy of Ba

The transmission spectra of the laser is shown in Fig. 2. The central absorption peak is due to the even isotopes of Ba, mainly ^{138}Ba which accounts for 70% of natural Ba with an addition of ^{136}Ba (6%), ^{134}Ba (2%) and ^{132}Ba (1%). Since the nuclear spin for all even isotopes is zero, there is no hyperfine structure. Natural Ba also contains relatively small amount odd isotopes ^{137}Ba (10%) and ^{135}Ba (10%), which are responsible for the adjacent absorption peaks in Fig. 2. Since the nuclear spin of the odd isotopes is $I = 3/2$, we observe three resolved absorption lines corresponding to the resonant transition to the excited hyperfine states with $F' = 1/2, 3/2, \text{ and } 5/2$.

It has been demonstrated that extremely narrow resonances may be observed in Ba atoms using saturation absorption spectroscopy [18, 19]. In our experiments, we also record Doppler-free spectra in the Ba vapor cell, but mainly for isotope identification and frequency calibration.

The part of the laser beam reflected from the polarizer P_1 is used as a counterpropagating pumping beam. The ratio between pump and probe field intensities is controlled by the half-wave plate placed before P_1 , and the

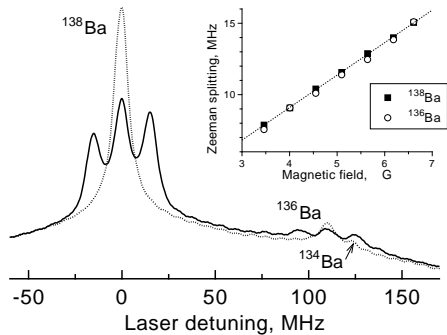


FIG. 3: Saturated absorption resonances at zero magnetic field (dotted line) and $B = 7.5$ G (solid line). *Inset*: Measured shift between the resonances as a function of magnetic field.

polarization of the pump beam may be changed by half- or quarter-wave plates placed after the polarizer. The width (FWHM) of the observed resonances is ≈ 8 MHz, which is determined by the spectral width of the laser radiation and residual Doppler effect. It is also interesting that the amplitude of the observed resonances shows no dependence on the polarization of the pumping beam. The positions of the transmission peaks are in very good agreement with previously published data [20].

We also study the Zeeman shift of the magnetic sublevels of the excited states in the presence of a longitudinal magnetic field. It is easy to calculate that for even isotopes the gyromagnetic ratio of the 3P_1 state is $g = 3/2$, which corresponds to a 2.11 MHz/G shift of the magnetic sublevels [21]. We have measured the splitting of the saturation absorption resonances as a function of applied magnetic field. The results are shown in Fig. 3. This method provides an accurate calibration of the magnetic field in the system. We also detected the Zeeman splitting for the transitions of the odd isotopes. However, individual magnetic resonances are not clearly resolved there due to the rich magnetic substructure of the hyperfine levels.

B. Nonlinear magneto-optical effects

Let us first consider the case when the magnetic field is applied along the propagation direction of the laser beam (Faraday configuration). The spectra of the polarization rotation angle for different magnetic fields are shown in Fig. 4. One can clearly see two different regimes: for smaller values of magnetic field ($B \leq 2$ G) the rotation spectrum consists of one peak, whereas for higher magnetic fields it becomes almost antisymmetric with respect to the center of the absorption line.

This behavior may be partially explained if we assume that for small magnetic field the nonlinear magneto-optical rotation is observed, and for higher B the linear interaction becomes dominant. We can check this hypothesis by looking at the dependence of the polar-

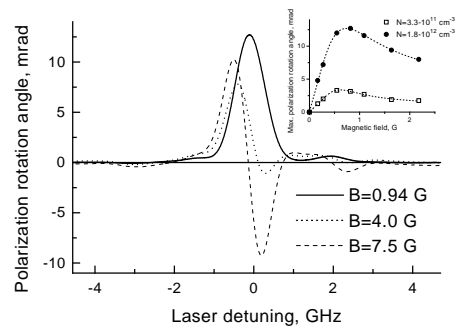


FIG. 4: The polarization rotation angle of linearly polarized light tuned across the Ba resonance for different values of the longitudinal magnetic field. The laser power is 2.2 mW, the density of Ba vapor is 1.8×10^{12} cm^{-3} . *Inset*: maximum polarization rotation angle as a function of magnetic field. Only the range of the magnetic fields where the nonlinear Faraday effect dominates is shown. The dotted lines are to guide the eyes.

ization rotation angle on the laser power in both cases. Nonlinear polarization rotation is caused by the light-induced coherence between the $m = \pm 1$ sublevels of the excited state, and therefore the magnitude of the rotation angle should depend on the light intensity. This will be shown in the next Section. Measurements of the rotation angle, shown in Fig. 5a are in good agreement with this statement. This also means that in some cases (for example, when the atomic transition is weak) it may be more convenient to study atomic transitions with NMOE spectroscopy than by absorption spectroscopy.

The linear Faraday effect, in which the polarization rotation is determined by the dispersion of the atomic transition, should not demonstrate any dependence on laser intensity. Fig. 5b shows the amplitudes of both rotation peaks in the linear regime. One can see that the amplitude of the positive peak does not change at all, whereas that of negative peak reduces a little as the laser power increases. This variation may be due to residual nonlinear Faraday effect. Overall, the behavior of the rotation angle indicates that the polarization rotation for high magnetic field is due to the linear interaction. However, there is no clear explanation of the antisymmetric shape of the rotation spectra. It is conceivable that it may be due to the influence of other even isotopes, even though there is no clear physical reasons why they cause the polarization rotation in the opposite direction, or of the magnitude comparable with that of ^{138}Ba .

It is also important to note that in the regime of nonlinear interaction we observe suppression of absorption for small values of magnetic field. This is a manifestation of Electromagnetically Induced Transparency [22, 23, 24] due to the Zeeman coherence created on the excited states magnetic sublevels. The absorption spectra for different values of magnetic field are shown in Fig. 6. One can also see that no change in the laser absorption occurs in the linear interaction regime.

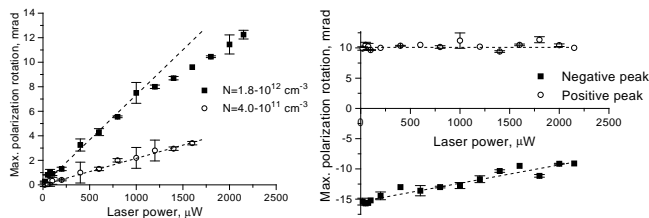


FIG. 5: (a) Maximum polarization rotation angle due to the nonlinear Faraday effect as a function of laser power. The data are taken at a magnetic field of $B = 0.9$ G for two values of atomic density. (b) The maximum values of the rotation peaks as functions of laser power for the linear interaction regime ($B = 7.5$ G). The density of Ba vapor is $1.8 \times 10^{12} \text{ cm}^{-3}$.

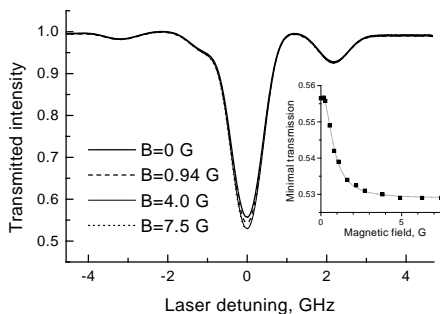


FIG. 6: Transmission through the cell for different values of magnetic field. *Inset*: Laser transmission on resonance as a function of magnetic field. Dotted line is a Lorentzian fit with FWHM of 1.7 G. The laser power is 2.2mW, the atomic density is $1.8 \times 10^{12} \text{ cm}^{-3}$.

We have also investigated the nonlinear magneto-optical polarization rotation in the presence of a transverse magnetic field. The magnetic field is applied perpendicular to both the electric component of the electromagnetic field and its propagation direction (along the z axis). The polarization rotation spectra is shown in Fig. 7. The magnitude of the polarization rotation is almost an order of magnitude smaller than that for the nonlinear Faraday effect. The other important difference is that the dependence of the rotation angle on the magnetic field is symmetric in the case of the transverse magnetic field, and asymmetric for the longitudinal magnetic field (not shown in the graphs).

To verify the nonlinear nature of the observed polarization rotation, we have measured the dependence of the polarization rotation on the laser intensity. As one can see in Fig. 8, the rotation angle is proportional to the power of the electromagnetic field, although this dependence is not linear.

Because of the symmetry of the system, a magnetic field applied parallel to the polarization direction of the linearly polarized magnetic field (the x -axis) should not produce any rotation. In the experiment, we observe some small (< 0.5 mrad) rotation angle in the presence of magnetic field along the x -axis, probably due to mis-

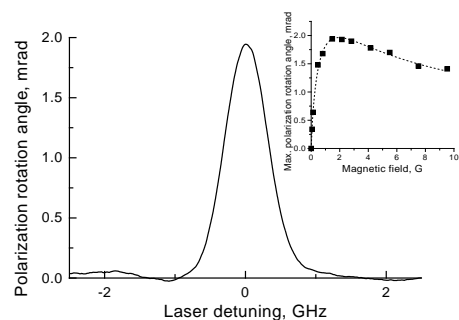


FIG. 7: The polarization rotation angle of linearly polarized light as a function of the laser detuning for transverse magnetic field $B_z = 2.0$ G. The laser power is 2.2 mW, the density of Ba vapor is $1.8 \times 10^{12} \text{ cm}^{-3}$. *Inset*: maximum polarization rotation angle as a function of magnetic field. The dotted lines are to guide the eyes.

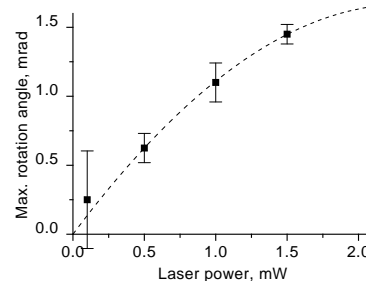


FIG. 8: Maximum polarization rotation angle for the case of transverse magnetic field as a function of laser power. The data are taken for magnetic field $B_z = 1.8$ G. The density of Ba vapor is $1.8 \times 10^{12} \text{ cm}^{-3}$. The dotted line is to guide the eyes.

alignment in the experimental apparatus.

III. THEORETICAL ANALYSIS

The level scheme of the Ba transition is shown in Fig. 9. Two components of the linearly polarized light link the ground state $|m = 0\rangle$ and two excited states $|m' = \pm 1\rangle$ into a V configuration; the third magnetic sublevel of the excited state cannot be excited because of the selection rules. We call the detuning of the laser from the atomic resonance Δ , and the Zeeman splitting of the magnetic sublevels of the excited states δ . Then the interaction Hamiltonian for this system in the rotating wave approximation is given by:

$$H = \hbar(\Delta - \delta)|-\rangle\langle -| + \hbar(\Delta + \delta)|+\rangle\langle +| - \hbar(\Omega_+|+\rangle\langle 0| + \Omega_-|-\rangle\langle 0| + \text{h.c.}) \quad (2)$$

Here and for the remainder of this discussion we let the states $|\pm\rangle$ and $|0\rangle$ refer correspondingly to the magnetic sublevels of the excited states $m' = \pm 1$ and the ground state with $m = 0$.

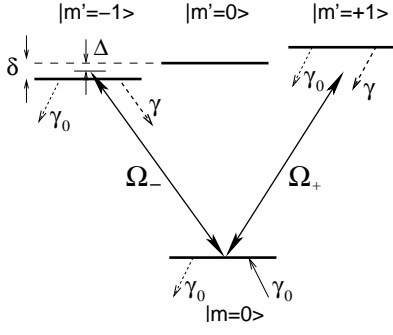


FIG. 9: The interaction scheme of a linearly polarized electromagnetic field with Ba atoms in the presence of a longitudinal magnetic field.

Using the hamiltonian (2), we write the Bloch equations for the density matrix elements

$$\dot{\rho}_{00} = \gamma_0(1 - \rho_{00}) + \gamma_r(\rho_{++} + \rho_{--}) + i(\Omega_+^* \rho_{+0} + \Omega_-^* \rho_{-0} - c.c.) \quad (3)$$

$$\dot{\rho}_{\pm\pm} = -(\gamma_0 + \gamma_r + \tilde{\gamma}_r)\rho_{\pm\pm} - i(\Omega_{\pm}^* \rho_{\pm 0} - \Omega_{\pm} \rho_{0\pm}) \quad (4)$$

$$\dot{\rho}_{\pm 0} = -\Gamma_{\pm 0} \rho_{\pm 0} + i\Omega_{\pm}(\rho_{00} - \rho_{\pm\pm}) - i\Omega_{\mp} \rho_{\pm\mp} \quad (5)$$

$$\dot{\rho}_{+-} = -\Gamma_{+-} \rho_{+-} + i\Omega_+ \rho_{0-} - i\Omega_+^* \rho_{+0} \quad (6)$$

where the polarization decay rates are given by:

$$\Gamma_{\pm 0} = (\gamma_0 + \gamma_r/2 + \tilde{\gamma}_r/2) + i(\Delta \pm \delta) \quad (7)$$

$$\Gamma_{+-} = (\gamma_0 + \gamma_r + \tilde{\gamma}_r) + i \cdot 2\delta \quad (8)$$

Here γ_r is the radiative decay rate of the excited states $m = \pm 1$ to the ground state, $\tilde{\gamma}_r$ is the decay outside of the three-level system, γ_0 characterizes the finite interaction time of the atoms with the laser beam. In the following calculations, we assume that γ_0 is small compared to γ_r , and define $\gamma = \gamma_r + \tilde{\gamma}_r$ as the total radiative decay rate of the excited states. For simplicity, we neglect the effect of spontaneous emission-induced coherent effects [25].

After solving Eqs. (3-6) in the steady-state regime, we obtain the following expression for the polarization

$$\rho_{\pm 0} = \frac{i\Omega_{\pm} (\Gamma_{\pm\mp} + \frac{|\Omega_{\pm}|^2}{\Gamma_{0\mp}})(\rho_{00} - \rho_{++}) - \frac{|\Omega_{\mp}|^2}{\Gamma_{0\mp}}(\rho_{00} - \rho_{++})}{\Gamma_{\pm 0} + \frac{|\Omega_{\pm}|^2}{\Gamma_{0\mp}} + \frac{|\Omega_{\mp}|^2}{\Gamma_{\pm 0}}} \quad (9)$$

Let us first briefly consider the linear interaction regime, such that magneto-optical effects do not depend on the intensity of the electromagnetic field and are determined solely by the resonant absorption and dispersion of the two-level interaction. From Eq. (9) it is easy to see that this regime is observed either for low intensity of the laser field ($|\Omega_{\pm}| \ll \gamma$), or for strong magnetic field ($\delta \gg |\Omega_{\pm}|, |\Omega_{\pm}|^2/\gamma$). In this case no coherence between excited states is created. The populations of the excited magnetic sublevels are determined by Rabi frequencies of the corresponding circularly polarized electro-magnetic

fields, and are small compared to the ground-state population. Thus, the propagation equation for the circular components of the laser field is:

$$\frac{\partial \Omega_{\pm}}{\partial z} = -\frac{\kappa \Omega_{\pm}}{\gamma/2 + i(\Delta \pm \delta)} \quad (10)$$

where $\kappa = \frac{3}{8\pi} N \lambda^2 \gamma_r$, and $|\Omega|^2 = |\Omega_+|^2 + |\Omega_-|^2$ is the total intensity of the electromagnetic field. Substituting $\Omega_{\pm} = |\Omega_{\pm}| \exp i\phi_{\pm} m$ and taking the real part of Eq. (10) we arrive at expressions for the absorption coefficient α (defined as $|\Omega(L)|^2 = |\Omega(0)|^2 e^{-\alpha L}$, where $|\Omega(L)|$ and $|\Omega(0)|$ are the values of the Rabi frequencies of the laser field before and after the cell)

$$\alpha = \kappa \gamma \frac{\gamma^2/4 + \Delta^2 + \delta^2}{(\gamma^2/4 + \Delta^2 + \delta^2)^2 - 4\Delta^2 \delta^2} \quad (11)$$

The polarization rotation angle is given by half the difference between the acquired phases of the circularly polarized fields $\phi = (\phi_+ - \phi_-)/2$. In case of the linear Faraday effect it is equal to

$$\phi = \kappa \delta L \frac{\gamma^2/4 - \Delta^2 + \delta^2}{(\gamma^2/4 + \Delta^2 + \delta^2)^2 - 4\Delta^2 \delta^2} \quad (12)$$

As one can see, Eq. (12) is symmetric with respect to the laser detuning Δ and therefore does not explain the dispersion-like curves observed in the experiment. However, this theoretical analysis is not complete without taking into account the velocity distribution of moving Ba atoms. It is known that in the hot vapor the atomic velocities are described by a Maxwell distribution: $dN\{v\} = N \exp(-v^2/v_T^2) dv$, where $v_T = \sqrt{2k_B T/m}$ is the most probable velocity, k_b is the Boltzmann constant, T is the temperature of atomic vapor in K, and m is the mass of a Ba atom. Because of the Doppler effect, the atoms from different velocity groups resonate at different frequencies. To account for this in our calculations it is necessary to modify Eq. (10) by replacing the one-photon detuning Δ with $\Delta + kv$, where $k = 2\pi/\lambda$ is the wave vector of the electromagnetic field, and then averaging the right-hand side of Eq. (10) over the velocity distribution.

The nonlinear magneto-optical effects appear due to the coherence which may be created among the Zeeman sublevels of the excited state. Unlike a three-level Λ system, where the ground-state coherence arises from optical pumping of the atoms in the noninteracting superposition of two ground-states (the “dark state”), in a V scheme the coherence between the two excited states is formed by the interference of different excitation passes [22].

In the approximation of strong electromagnetic field ($|\Omega| \gg \gamma$) we may assume that the population distribution in the system is determined mostly by the field. Therefore, we can assume that the atom is in one of the eigenstates of the Hamiltonian (2), which allow us to find the values of the populations of all levels in zeroth ap-

proximation. It is quite easy to find this state for $\delta = 0$:

$$|\Psi\rangle = \mathcal{N} \left\{ \Omega_+^* |+\rangle + \Omega_-^* |-\rangle - \left(\frac{\Delta}{2} + \sqrt{\frac{\Delta^2}{4} + |\Omega|^2} \right) |0\rangle \right\} \quad (13)$$

where the normalization coefficient \mathcal{N} is given by

$$\frac{1}{\mathcal{N}^2} = 2\sqrt{\frac{\Delta^2}{4} + |\Omega|^2} \left(\frac{\Delta}{2} + \sqrt{\frac{\Delta^2}{4} + |\Omega|^2} \right). \quad (14)$$

In this case we find the population differences between the excited states and the ground state are the following:

$$\rho_{00}^{(0)} - \rho_{\pm\pm}^{(0)} = \mathcal{N}^2 \left\{ \frac{\Delta^2}{2} + \Delta \sqrt{\frac{\Delta^2}{4} + |\Omega|^2} + |\Omega_{\mp}|^2 \right\}. \quad (15)$$

Substituting the expressions for atomic populations above into Eq. (9) we may find the values of atomic polarizations in the approximation $|\Omega| \gg \delta, \gamma, \Delta$

$$\rho_{\pm 0} \simeq i\Omega_{\pm} \frac{(\gamma + 2i\delta - 2i\Delta)|\Omega_{\mp}|^2}{|\Omega|^4}. \quad (16)$$

Using Eq. (16) it is easy to calculate the transmitted intensity and the polarization angle of the linearly polarized electromagnetic field

$$|\Omega(L)|^2 = |\Omega(0)|^2 - \kappa\gamma L \quad (17)$$

$$\phi = \frac{2\delta}{\gamma} \ln \frac{|\Omega(0)|^2}{|\Omega(L)|^2} \quad (18)$$

This result is in a good agreement with the previous calculations [5] in the limit of optically thin medium. Note that this expression is very similar to that for the Λ system [26] with the decay rate of the ground-state coherence replaced by the radiative decay of the excited states.

From Eq. (18) one can see that the polarization rotation angle is inversely proportional to the radiative width of the excited state. Therefore, it is clear that several orders of magnitude may be gained in polarization rotation

and other nonlinear effects in V interaction scheme by using narrow alkaline-earth intercombination transitions compared with traditional alkali atoms.

It is easy to see, however, that the theory developed above predicts much larger values of the polarization rotation angle than experimentally observed. There are several effects which may contribute to this discrepancy. For example, we do not take into account thermal motion of atoms which, from one hand, leads to the inhomogeneous Doppler broadening, and from the other hand - limits the interaction time of Ba atoms with light. Indeed, the average thermal speed of Ba atoms at about 500° C is about 300 m/s, which corresponds to a decay rate $\gamma_0 \approx 2\pi \times 50$ kHz and is comparable with the radiative width of the transition. This may change the population distribution between atomic levels. Another important factor is the presence of relatively dense ($> 10^{13}$ cm $^{-3}$) Rb vapor due to small contamination of Ba sample, since it has been demonstrated that collisions cause the reduction of the polarization rotation [5].

IV. SUMMARY

In this paper, we have presented an experimental study of linear and nonlinear optical effects on the intercombination transition 6S-6P of Ba atoms in sealed vapor cell. We study the Zeeman shift of the magnetic sublevels of the excited state and measure the polarization rotation spectra in presence of longitudinal and transverse magnetic fields. These nonlinear optical effects can have a wide range of applications as a spectroscopic tool with good resolution and sensitivity for studying weak atomic transitions.

V. ACKNOWLEDGEMENTS

The authors would like to thank E. E. Mikhailov, Y. Malakyan, V. A. Sautenkov, and A. S. Zibrov for useful and stimulating discussions, and Office of Naval Research for financial support.

-
- [1] D. Budker, W. Gawlik, D. F. Kimball, S. M. Rochester, V. V. Yashchuk, and A. Weis, *Rev. Mod. Phys.* **74**, 1153 (2002).
 - [2] K. H. Drake, W. Lange, and J. Mlynek, *Opt. Commun.* **66**, 315 (1988).
 - [3] L. M. Barkov, D. A. Melik-Pashaev, and M. S. Zolotarev, *Opt. Commun.* **70**, 467 (1989).
 - [4] G. S. Agarwal, P. A. Lakshmi, J. P. Connerade, and S. West, *J. Phys. B* **30**, 5971 (1997).
 - [5] F. Schuller, M. J. D. Macpherson, and D. N. Stacey, *Physica C* **147**, 321 (1987).
 - [6] F. Schuller, R. B. Warrington, K. P. Zetie, M. J. D. Macpherson, and D. N. Stacey, *Opt. Commun.* **93**, 169 (1992).
 - [7] F. Schuller and D. N. Stacey, *Phys. Rev. A* **60**, 973 (1999).
 - [8] A. S. Zibrov, M. D. Lukin, D. E. Nikonov, L. Hollberg, M. O. Scully, V. L. Velichansky, and H. G. Robinson, *Phys. Rev. Lett.* **75**, 1499 (1995).
 - [9] G. Grynberg, M. Pinard, and P. Mandel, *Phys. Rev. A* **54**, 776 (1996).
 - [10] P. Zhou and S. Swain, *Phys. Rev. Lett.* **78**, 832 (1997).
 - [11] A. M. Akulshin, S. Barreiro, and A. Lezama, *Phys. Rev. A* **57**, 2996 (1998).
 - [12] A. V. Taichenachev, A. M. Tumaikin, and V. I. Yudin, *Phys. Rev. A* **61**, 011802 (2000).
 - [13] G. Alzetta, S. Cartaleva, Y. Dancheva, C. Andreeva, S. Gozzini, L. Botti, and A. Rossi, *J. Opt. B* **3**, 181 (1999).

- (2001).
- [14] A. N. Nesmeyanov, *Vapour Pressure of the Elements* (Academic Press, New York, 1963).
- [15] E. Hinnov and W. Ohlendorf, *J. Chem. Phys.* **50**, 3005 (1969).
- [16] C. B. Alcock, V. P. Itkin, and M. K. Horrigan, *Canadian Metallurgical Quarterly* **23**, 309 (1984).
- [17] K. T. Jacob and Y. Waseda, *J. of the Less-Common Metals* **139**, 249 (1988).
- [18] A. M. Akulshin, A. A. Celikov, and V. L. Velichansky, *Opt. Commun.* **93**, 54 (1992).
- [19] R. Loe-Mie, A. V. Papoyan, A. M. Akulshin, A. Lazema, J. R. R. Leite, O. Lopez, D. Bloch, and M. Ducloy, *Opt. Commun.* **139**, 55 (1997).
- [20] P. Grundevik, M. Gustavsson, G. Olsson, and T. Olsson, *Z. Phys. A* **312**, 1 (1983).
- [21] I. I. Sobel'man, *Introduction to the theory of atomic spectra* (Pergamon Press, Oxford, 1972).
- [22] M. O. Scully and M. S. Zubairy, *Quantum Optics* (Cambridge University Press, Cambridge, UK, 1997).
- [23] S. E. Harris, *Phys. Today* **50**, 36 (1997).
- [24] J. P. Marangos, *J. Mod. Opt.* **45**, 471 (1998).
- [25] E. Paspalakis, S.-Q. Gong, and P. L. Knight, *Opt. Commun.* **152**, 293 (1998).
- [26] A. B. Matsko, I. Novikova, M. S. Zubairy, and G. R. Welch, *Phys. Rev. A* **67**, 043805 (2003).